Pressure-induced polymerization of C_{60} at high temperatures: An *in situ* Raman study

A. V. Talyzin,[1] L. S. Dubrovinsky,[2] T. Le Bihan,[3] and U. Jansson[1]
[1]*Department of Materials Chemistry, Ångström Laboratory, Box 538, SE-751 21, Uppsala, Sweden*
[2]*Bayerisches Geoinstitut, Universität Bayreuth, D-95440 Bayreuth, Germany*
[3]*European Synchrotron Radiation Facility, Grenoble 38043, France*
(Received 16 April 2001; revised manuscript received 21 June 2001; published 29 May 2002)

In situ Raman spectroscopy data of C_{60} polymerization under high-temperature–high-pressure conditions are presented. We have studied a diagonal section of the *P-T* diagram starting from room temperature and a pressure of 5.5 GPa, heating the sample up to 780 K and 1.5 GPa, followed by a cooling of the sample back to room temperature and a pressure of 7.5 GPa. Only known one- and two-dimensional polymeric phases of C_{60} were observed. X-ray diffraction from a quenched sample obtained with synchrotron radiation showed that it consists of a mixture of orthorhombic and tetragonal phases with a small addition of rhombohedral phase. A *P-T* diagram based on our *in situ* data is in good general agreement with similar diagrams constructed from *ex situ* studies data.

DOI: 10.1103/PhysRevB.65.245413 PACS number(s): 61.48.+c, 62.50.+p, 61.50.Ks

I. INTRODUCTION

It is well known that a high-pressure–high-temperature treatment (HPHT) of C_{60} below 9 GPa and 900 K leads to the formation of several kinds of one- and two-dimensional polymers,[1–5] while three-dimensional polymers typically are formed at higher pressures.[6,7] Several different *P-T* diagrams have been published in the literature to describe the phase compositions at different temperatures in this pressure region ($<$9 GPa).[4,5,8] It is important to note that these diagrams are not phase diagrams since C_{60} is a metastable modification of carbon, and the term ''equilibrium phases'' should not be used. The published diagrams exhibit some similarities but also some important differences. This can only partly be explained by differences in the experimental procedures (use of hydrostatic or nonhydrostatic pressure, variation in heating times, applied analysis technique, etc.). For example, Sundqvist[5] reported that a chainlike orthorhombic phase is formed at moderate temperatures ($>$350 K) and the pressure range 1–8 GPa. In contrast, Davydov *et al.* recently reported that a dimeric phase is formed at room temperature at pressures above 1 GPa,[4] and their observations of orthorhombic phase have been limited to pressures below 2 GPa. Furthermore, an x-ray-diffraction study by Bennington *et al.*[9] also showed no orthorhombic phase for 2.6 and 5.7 GPa. A general observation, however, is that two-dimensional polymers with a rhombohedral or tetragonal structure have been found to form at temperatures above 500–600 K.[4,5,9] The stability regions for these phases are unclear and differ from one investigation to another, but the rhombohedral phase seems to be favored by a higher pressure. Some studies showed also multiphase regions in the *P-T* diagrams.[5,10] The published *P-T* diagrams also show that monomeric, unpolymerized C_{60} is stable at low pressures and high temperatures. Today, Raman spectra have been recorded for all one- and two-dimensional polymeric phases, and characteristic features of the spectra have been identified for each phase. Some of the most typical signatures for polymerization are (i) a shift of the $A_g(2)$ mode originally found at 1469 cm^{-1}, proportional to a number of square rings connecting neighboring C_{60} molecules; (ii) peaks originating from square ring vibrations around 900–1000 cm^{-1}, and (iii) peaks below 200 cm^{-1} due to intercage vibrations.[4,5,8]

A problem with all previous Raman HPHT studies is that they have been carried out *ex situ*. This means that the samples have been heated and pressurized, and then quenched (cooled down and pressure released). Characterization with a suitable analysis technique has then been carried out at room temperature and normal pressure. A problem with this procedure is that the phase composition can be changed during quenching. There are numerous examples where high-pressure phases can be observed *in situ* at HPHT conditions but not observed *ex situ* in quenched samples (e.g., of Fe, TiO_2, and $CaSiO_3$). Recently in our laboratory we also observed that pressurized thin-film-samples of C_{60} change phase composition during the quenching procedure.[11] Furthermore, the heating may also change the pressure inside a compressed volume due to technical reasons. *Ex situ* studies leave this aspect impossible to evaluate and may give rise to erroneous data points in a *P-T* diagram. Finally, it must also be noted that most of the studies used by Sundqvist to construct the *P-T* diagram for C_{60} were obtained using hydrostatic conditions. Nonhydrostatic pressure conditions have been shown to produce polymerization of C_{60} even at room temperature at pressures above approximately 7 GPa.[12]

From the discussion above, it is clear that *in situ* studies are required to determine the phase compositions at true HPHT conditions. Hitherto, technical problems have restricted *in situ* Raman studies of C_{60} at high pressures to room temperature. In this work, however, we present the first true *in situ* Raman study of C_{60} polymerization at HPHT and nonhydrostatic conditions. The *in situ* results are compared with previous *ex situ* studies.

II. EXPERIMENT

Powder samples of freshly sublimed C_{60} (99.95% purity, MER Corporation) were studied using the TAU-type diamond-anvil cell (DAC) (Ref. 13) with 250-μm flat culets without pressure transmitting medium. Powder of C_{60} and

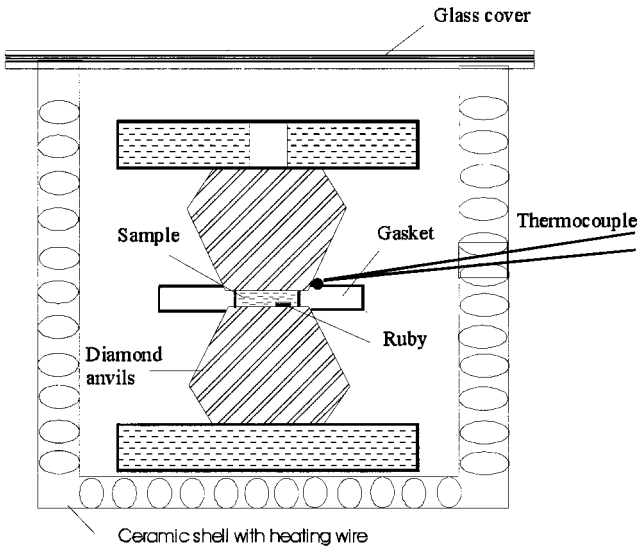

FIG. 1. Scheme of the experimental setup.

several 2–3-μm size ruby chips were loaded in the hole, 125 μm in diameter, drilled in a Re gasket. Initial thickness of the sample was 35 μm. The pressure variation at the maximum pressure (5.5 GPa) was ± 1 GPa within 100 μm of the central part of the sample. The Raman spectra were measured from the same spot close to the center of the sample. The diameter of the analysis area was less than 5 μm.

The cell was placed into a resistively heated ceramic shell with a glass window and a nitrogen flow was used inside the heater to prevent cell oxidation; see Fig. 1. The temperature was controlled by a *K*-type thermocouple inserted inside the cell at the diamond-gasket interface. Pressure was measured using the ruby fluorescence scale corrected for temperature effects.[14] In the HPHT experiments, the samples were pressurized to 5.5 GPa and heated slowly to 780 K step by step. During the heating-cooling cycle, Raman spectra were recorded using short measurement times at every 10 K. At every 100 K, the temperature was allowed to stabilize for 10–20 min and Raman spectra were recorded using longer acquisition times (30–60 min). It must be noted, however, that at the highest temperatures (around 780 K) the heating time was reduced (10–15 min) in order to decrease the risk of cell damage. The total cycle time for an experiment was about 9 h. After completion of the heating-cooling cycle the pressure in the cell was found to be 7.5 GPa. This is about 2 GPa higher than the initial pressure, and shows that some pressure changes have occurred during the experiment. The variations of the pressure during an experiment are related to a mechanical relaxation of the DAC.

A Renishaw Raman 2000 spectrometer with 514- and 785-nm lasers was used in the experiments. Raman spectra were recorded *in situ* during a heating-cooling cycle through the diamond anvils using a long focus 50$\times$ objective. With such an objective the studied area is approximately 5 μ in the focal plane, and the depth of the focus is less than 10 μm. *Ex situ* spectra were also obtained from quenched samples. During the heating-cooling cycle, the 785-nm laser was used for spectra recording, since it provided a much better signal-to-noise ratio than the 514-nm laser and therefore made it possible to record acceptable spectra with rather short acquisition times. Before and after heating, as well as after quenching, spectra were also recorded with the 514-nm laser, since this wavelength was used in the most of the studies presented in the literature. The resolution was 2 cm^{-1} in all of our experiments. The PEAKFIT software was used for fitting of spectra with Voigt functions after background subtraction. It shall be noted that below approximately 400–500 cm^{-1} the quality of the spectra was less good due to interference effects.

Precise pressure calibration turned out to be a difficult problem since the ruby luminescence peaks were weak with the 785-nm laser, especially at high temperatures. Therefore, separate experiments were performed using the 514-nm laser. This experiment showed a linear decrease of the pressure with increasing temperature. At about 800 K the pressure decreased at approximately 3–4 GPa. We also found that the position of the diamond peak (at around 1332 cm^{-1} at RTP) originating from the anvils can be used for monitoring pressure during the heating. The diamond peak position was found to shift linearly with temperature. For pressure and temperature calibration of the diamond peak we need two reference points with a known temperature and pressure. The two reference points were set to 293 K 5.5 GPa and 780 K 1.5 GPa, respectively. With a knowledge of the temperature in every point of our measurements and using the shift of the diamond peak relative to the reference two points, we can assign each Raman spectrum to a certain point in a *P-T* diagram for C_{60}.

Two-dimensional (2D) x-ray-diffraction patterns of the quenched samples were taken in transmission geometry on the ID30 beamline at the European Synchrotron Radiation Facility (ESRF, Grenoble, France) with the MAR345 detector using an x-ray beam of 0.3738-Å wavelengths and a size of 20×10 μm^2. The Detector-to-sample distance was 350 mm. The collected images were integrated using the FIT2D program in order to obtain a conventional diffraction spectrum.

III. RESULTS AND DISCUSSION

A. General observations

As can be seen in Fig. 2(a), a room-temperature Raman spectrum of a sample pressurized to 5.5 GPa is slightly different compared to the pristine C_{60} spectrum. An asymmetric shape of the $A_g(2)$ mode and a strong change in relative intensity of some peaks indicate that a fraction of polymeric phase (dimers or chains) is already present at room temperature. The spectra in Fig. 2 also show the appearance of a number of new peaks at higher temperature. This indicates that the degree of polymerization increases as a function of temperature. Surprisingly, however, a maximum in polymerization can be seen at about 670 K. A further increase in temperature leads to the reverse process, and at 780 K all polymers have decomposed and the Raman spectrum is very similar to that of pure, unpolymerized C_{60} [see Fig. 2(b)]. The decomposition of the polymeric phases at high temperatures can easily be explained by the fact that the pressure during heating is reduced (see Sec. II). It is known that C_{60}

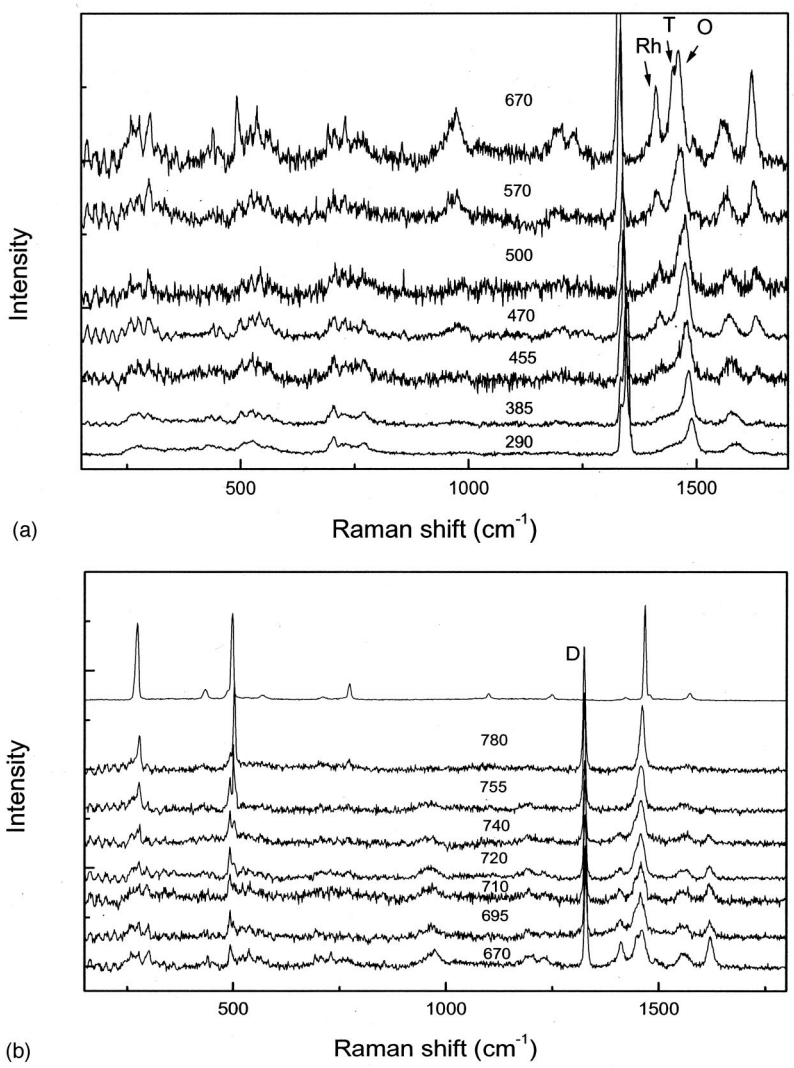

FIG. 2. *In situ* Raman spectra recorded during the heating for two temperature intervals: (a) 290 K (5.5 GPa)–670 K (2.3 GPa) and (b) 670 (2.3 GPa)–780 K (1.5 GPa). The top spectrum in (b) is recorded from pristine C_{60} *ex situ* at ambient conditions.

polymers depolymerize at ambient pressure if heated to 400–500 K.[15] We know from our experiments that the pressure at 780 K should be about 1.5 GPa (see Sec. II). It should also be noted that the phase diagram recently published by Sundqvist and co-workers shows that the one and two-dimensional polymeric C_{60} phases will decompose to monomeric C_{60} at about 1–1.5 GPa at 780–800 K.[5,8,16]

From the results above we can conclude that we not have made a vertical section in the *P-T* diagram but rather a diagonal section connecting room temperature and 5.5 GPa with our reference point at 780 K and 1.5 GPa. Also, during cooling we observed a linear increase of the pressure. Down to approximately 520 K the pressure increased very closely to the pathway observed during the heating. Below this temperature, the actual pressure during cooling was higher compared to corresponding point on the heating curve leading to a final pressure of 7.5 GPa.

B. Raman analysis during heating

The spectra obtained during heating and cooling show some differences, and will therefore be discussed separately. As mentioned above, the heating experiments show an initial polymerization, which achieved a maximum at 670 K followed by decomposition of polymeric C_{60} to the monomeric phase. Different polymers of C_{60} can be identified by comparing the $A_g(1)$ and $A_g(2)$ modes at different temperatures, as shown in Figs. 2(a) and 2(b). A problem with the interpretation of the spectra is that the shifts of the C_{60} peaks due to polymerization must be separated from shifts due to changes in pressure and temperature. A more precise determination of the phase composition is possible since it is known that the position of the $A_g(2)$ mode is downshifted by 5, 10, and 21 cm^{-1} for dimeric, one-dimensional orthorhombic, and two-dimensional tetragonal phases, respectively.[17] It is reasonable to suggest that the relative positions of these peaks remain similar under HPHT conditions, but a clear reference point is required since even at room temperature our sample is partly polymerized. As shown above the sample at 780 K and 1.5 GPa consists mainly of monomeric C_{60}. We have used the $A_g(2)$ peak of unpolymerized C_{60} at this temperature and pressure as a reference peak, and will therefore discuss the Raman spectra starting at the highest temperature and continue down to room temperature.

The monomeric C_{60} at 780 K is formed by a decomposition of a polymeric phase. At temperatures below 780 K, a

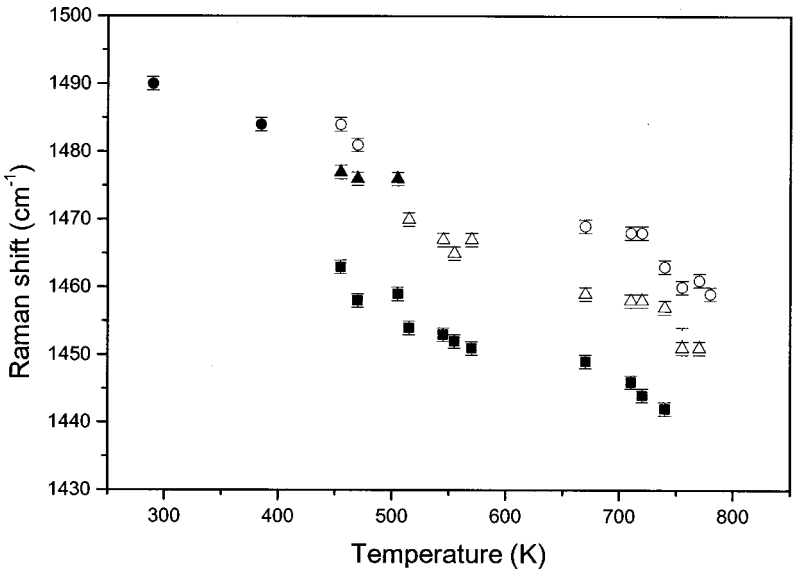

FIG. 3. Peak positions during the heating at different temperatures (and pressures, see the text) for $A_g(2)$ modes of the following phases: ○, monomeric; ●, mixture of monomeric and dimeric polymers; ▲, mixture of dimeric and chain polymers; △, orthorhombic (chainlike); ■, tetragonal (2D).

peak can be seen which is downshifted with about 10 cm^{-1} compared to the $A_g(2)$ mode of unpolymerized C_{60} [see Fig. 2(b)]. This peak can be attributed to a chain polymer with an orthorhombic structure.[4,8] The intensity of the orthorhombic peak clearly dominates the spectrum at 740 K, but is reduced at higher temperatures as the orthorhombic phase decompose into monomeric C_{60}. The depolymerization can be followed directly by comparing the relative intensities of the $A_g(1)$ modes at 500 cm^{-1}, which can be assigned to unpolymerized C_{60}, and the peak at about 490 cm^{-1} which can be assigned to the orthorhombic and tetragonal polymers.[4] As can be seen in Fig. 2(b), the intensity of the polymer peak is reduced with increasing temperature, and at 780 K the typical spectrum of monomeric C_{60} is observed. A small amount of orthorhombic phase is still present at this temperature but it decreases with increasing time of the high temperature treatment.

Below 740 K, a shoulder can be observed with a downshift of about 20 cm^{-1} compared to the $A_g(2)$ mode of unpolymerized C_{60}. This peak can be attributed to the two-dimensional tetragonal phase with four square rings per C_{60}. At 670 K and 2.3 GPa, the intensity of the tetragonal peak is more or less equal to the $A_g(2)$ peak from the orthorhombic phase. It should be noted that the positions of the $A_g(1)$ modes of the orthorhombic and tetragonal phases are similar, and that this mode therefore can not be used as a signature for these phases.[4] At this temperature it is also clear that a third phase is present in the sample. This phase has peaks at 1409, 729, and 1621 cm^{-1}, and can be assigned to a two-dimensional, rhombohedral phase described by, for example, Davydov *et al.*.[4] It should be noted that this phase, which should contain six square rings per C_{60} molecule, seems to fall outside the trend observed for the $A_g(2)$ mode peak shift. The pure rhombohedral phase claimed to be obtained in a recent study by Davydov *et al.*[4] exhibits an $A_g(2)$ peak at 1406 cm^{-1} at ambient conditions which would correspond to 12 square rings per molecule assuming a shift of 5 cm^{-1} per square ring. However, 12 square rings per C_{60} molecule require a three-dimensional polymerization although all other experimental data (e.g., x-ray diffraction, density measurements) show that this phase is a two-dimensional polymeric phase.

Figures 2(a) and 2(b) show that at 670 K and 2.3 GPa we have the highest degree of polymerization with a mixture of three phases: an orthorhombic chain polymer, a tetragonal two-dimensional polymeric phase, and a rhombohedral two-dimensional polymeric phase. The formation of this mixture during heating from room temperature can be followed in Fig. 2(a). At lower temperatures, the $A_g(2)$ mode can be attributed mainly to the monomeric phase (with addition of small amount of dimers), but above 470 K this feature is dominated by contributions from the orthorhombic and tetragonal phases. The formation of the rhombohedral phase can clearly be seen at about 450–470 K, and the relative intensity of the peaks from this phase increases up to 670 K. From the spectra in Figs. 2(a) and 2(b) it can be difficult to identify the individual contribution of the different phases to the $A_g(2)$ feature. A peak-fitting program was therefore used to resolve the different peaks in each spectrum, and the results are summarized in Fig. 3, where the peak positions for each phase (except the rhombohedral) are given as a function of temperature during the heating step. The plot shows that no monomeric phase is observed between about 470 and 670 K. According to literature data, the shifts of the orthorhombic and tetragonal $A_g(2)$ peaks relative to the $A_g(2)$ peak of the monomeric phase are 10 and 20 cm^{-1}, respectively [i.e., the shift of the $A_g(2)$ peaks between tetragonal and orthorhombic phase is about 10 cm^{-1}]. Figure 3 shows that this is the case in the temperature region 670–780 K. In contrast, a slightly different behavior can be observed between about 450 and 570 K. In this region the shift between the tetragonal and orthorhombic peaks is about 15 cm^{-1}. Furthermore, the downshift of the assumed orthorhombic $A_g(2)$ peak relative the monomeric peak is only about 5 cm^{-1}. These shifts are consistent with the formation of a dimeric phase. We therefore suggest that the sample between 450 and 570 K consists of a dimeric phase or more likely a mixture of the orthorhombic and dimeric chain polymer. The fraction of the

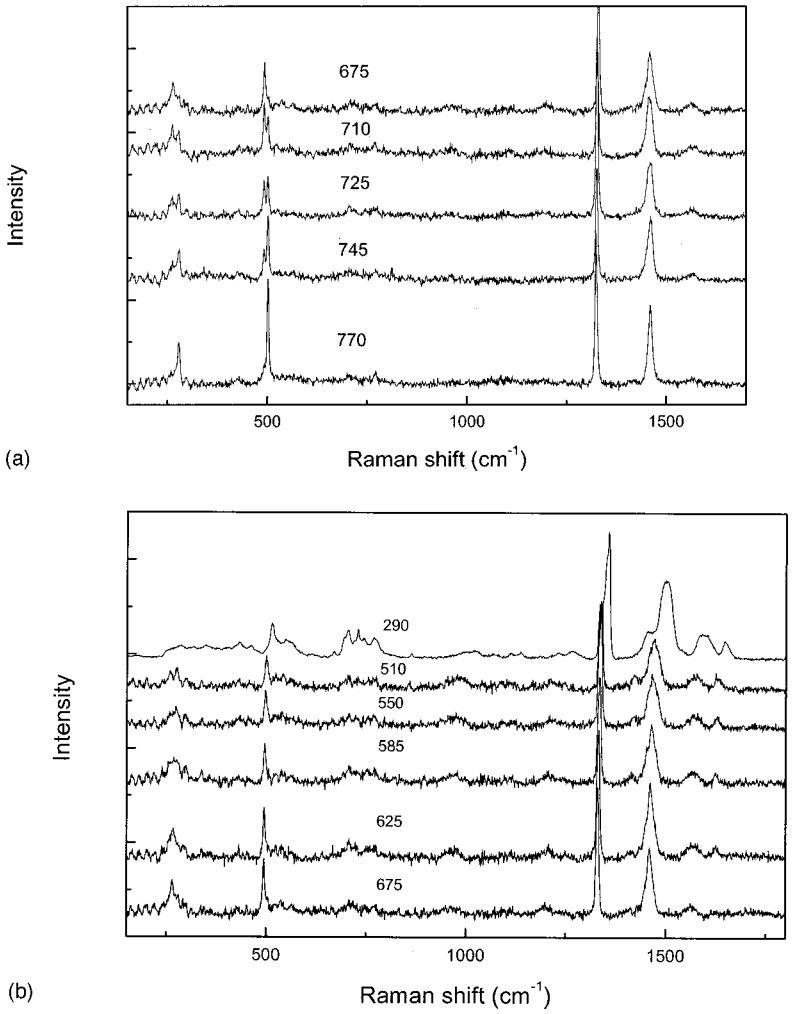

FIG. 4. *In situ* Raman spectra recorded during the cooling for temperature intervals: (a) 770 (1.5 GPa)–675 K (2.5 GPa) and (b) 675 (2.5 GPa)–290 K (7.5 GPa)

orthorhombic phase in this mixture increases at higher temperatures. The formation of the dimeric phase at low temperatures was previously reported in the literature by Davydov *et al.*[4] It should be noted that the dimeric phase has a typical intermolecular mode at 97 cm^{-1} (Ref. 9), which can be used as a fingerprint. Unfortunately, however, we have strong interference effects at this frequency range and have been unable to detect this mode as well as similar modes for other polymers.

In summary, the heating results show that dimeric and orthorhombic chain polymers initially are formed as the temperature is increased. Above 470 K, tetragonal and rhombohedral polymers can be seen in the spectra. At 670 K (2.3 GPa) (where the highest degree of polymerization is observed) we have a mixture of three phases: an orthorhombic one-dimensional chain polymer, a tetragonal two-dimensional polymer with four square rings per C_{60}, and a rhombohedral two-dimensional polymer with six square rings per C_{60}. It is also clear that heating from 670 K (2.3 GPa) to 780 K (1.5 GPa) leads to a depolymerization of first the rhombohedral phase, followed by the tetragonal phase, and finally the decomposition of the orthorhombic phase to monomeric C_{60}. Furthermore, the formation of two-dimensional phases also give rise to a number of additional peaks in the spectral region 200–800 cm^{-1}, and to a sharp increase in intensity of the peaks around 1000 cm^{-1}. The latter peaks have been assigned to vibrations of square rings connecting C_{60} molecules.[17] In our spectra we can clearly see that these peaks correlate well with the formation of the two-dimensional phases.

C. Raman analysis during cooling

The phase composition during the cooling step was different compared to the heating step. This shows that the polymerization sequence is not reversible within the time frames of our experiment. Figure 4(a) shows the Raman spectra recorded during cooling from 780 down to 675 K. As can be seen, the sample at 780 K (1.5 GPa) consists of mostly pure monomeric C_{60}, while at 675 K (2.3 GPa) it consist of mainly orthorhombic chain polymer. The transformation from monomeric phase to orthorhombic polymer can be seen as a downshift of the both $A_g(1)$ and $A_g(2)$ modes by 10 cm^{-1}. Especially clear this transformation can be observed for the $A_g(1)$ mode around 500 cm^{-1}. The intensity of the peak from the orthorhombic polymer increases during the cooling, while the intensity of the peak from the monomeric phase decreases. The same can be observed for $A_g(2)$ peaks which are less sharp and more overlapped, but can be resolved using fitting procedures. At 675 K, the sample con-

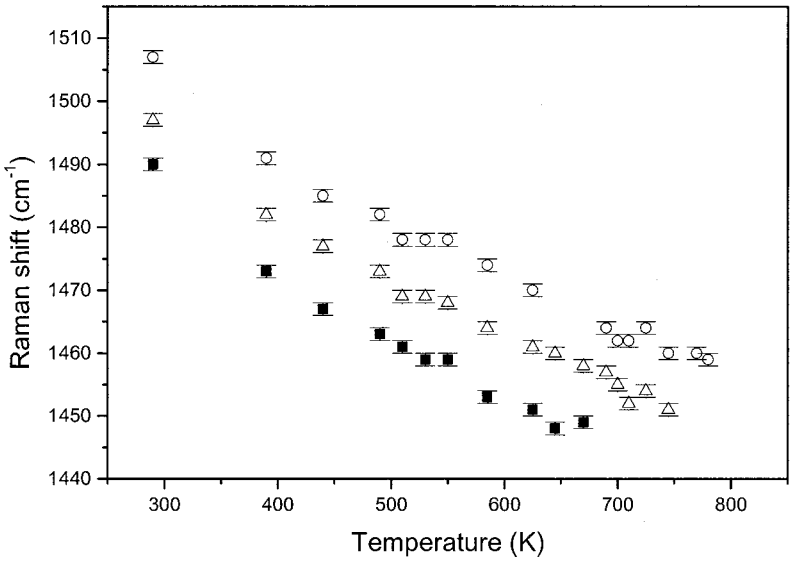

FIG. 5. Peak positions during the cooling at different temperatures (and pressures; see the text) for $A_g(2)$ modes of the following phases: ○, monomeric; △, orthorhombic (chainlike); ■ tetragonal (2D).

sists mainly of the orthorhombic phase but small amounts of monomeric C_{60} and tetragonal phases are also present. No indication of the rhombohedral phase can be seen at this temperature.

The second part [Fig. 4(b)] of the cooling step is from 675 K (2.3 GPa) to room temperature (7.5 GPa). Here we observe an increase in the amount of the tetragonal phase as well as the appearance of a small fraction of the rhombohedral phase. The highest degree of polymerization can be seen at 510–490 K. It must be noted, however, that the maximum intensities of the peaks from rhombohedral phase were several times lower during cooling compare to the heating run. During the final part of the cooling step from 510 K (5.6 GPa) to room temperature (7.5 GPa), only very small changes in the relative intensities of the peaks could be observed. This means that at room temperature and 7.5 GPa we have a mixture of mainly orthorhombic and tetragonal phases with a smaller amount of the rhombohedral phase. The monomeric C_{60} was also observed during the entire cooling step, but it decreased significantly and at room temperature was present only as a very small impurity. The shifts of the $A_g(2)$ modes of the monomeric, orthorhombic, and tetragonal phases calculated using a peakfitting procedures are shown in Fig. 5. As can be seen, the cooling data show a very stable correlation between the modes with a constant shift of 10 and 20 cm^{-1} of the orthorhombic and tetragonal modes, respectively, relative to the monomeric mode.

D. Raman spectroscopy of a quenched sample

Figure 6 shows an *in situ* Raman spectra from the sample after the heating-cooling cycle at room temperature and 7.5 GPa together with a spectra recorded after pressure release (quenching). Well-resolved peaks from the spectra recorded after pressure release are listed in Table I. A fitting of the spectra from the quenched sample in Fig. 7 shows that the most intense component of the $A_g(2)$ mode belongs to the orthorhombic phase (1460 cm^{-1}), followed by the tetragonal phase (1448 cm^{-1}), while less intense peaks of the rhombohedral phase are situated at 1410 and 1432 cm^{-1}. It is possible that the latter line can be a $H_g(7)$ mode from an ortho-

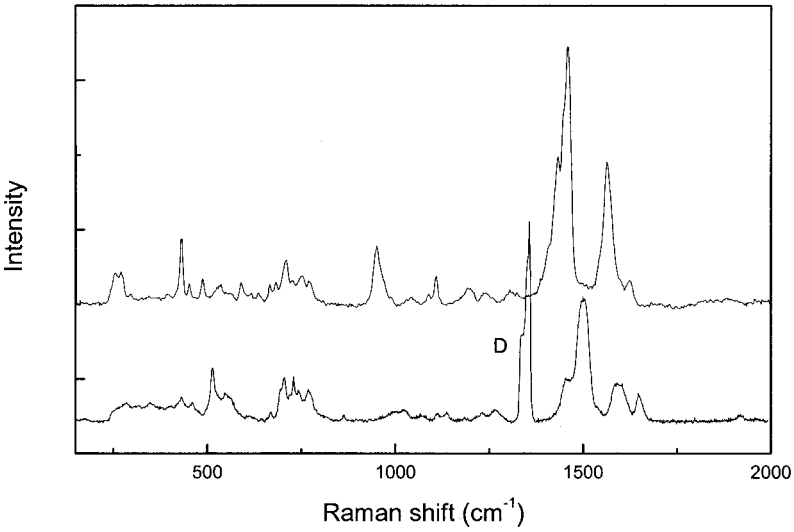

FIG. 6. Raman spectra of the quenched sample recorded *ex situ* (a) compared with *in situ* spectra of the sample after heating-cooling cycle at 290 K (b) Diamond peaks from anvils are labeled as *D*.

TABLE I. Peak positions observed in the Raman spectra of the sample after pressure release.

Raman shift, cm^{-1}	Assignment
1623	?
1565	$H_g(8)$
1469	$A_g(2)$ monomeric
1460	$A_g(2)$ orthorhombic
1448	$A_g(2)$ tetragonal
1432	$H_g(7)$?
1410	$A_g(2)$ rhombohedral
1314	?
1240	$H_g(6)$?
1196	?
1108	$H_g(5)$
1088	?
1042	?
971	Square
953	ring vibrations?
772	
751	
726	
708	$H_g(4)$- and
683	$H_g(3)$-derived modes
667	
637	
592	?
532	$F_1u(1)$?
488	$A_g(1)$
451	?
432	$H_g(2)$
395	?
296	
271	$H_g(1)$ derived
257	

rhombic or rhombohedral polymer, with a strongly increased intensity compared to fcc C_{60}. Peaks from monomeric C_{60} are very weak, which means that most of the sample is polymerized. These modes are also observed in the spectra recorded from the sample before pressure release, but they are less well resolved and look more like one broad peak. The peaks are also upshifted due to the higher pressure. A fitting of this peak gives positions of $A_g(2)$ modes from the monomeric, orthorhombic, and tetragonal phases at 1507, 1497, and 1490 cm^{-1} respectively, while peaks from the rhombohedral phase are observed at 1423 and 1456 cm^{-1}. The main difference between spectra recorded before and after pressure release is in the relative intensity of some peaks. Unfortunately, a direct comparison of intensity between the spectra is difficult since they are recorded with different lasers. A spectrum of the quenched sample could not be recorded with the 785-nm laser due to problems with a very high luminescence background. Nevertheless, we can see some clear differences between the spectra that cannot be due to the use of different lasers. The most remarkable observation is that the quenched spectrum has a clear and rather sharp feature at about 952 cm^{-1} that is assumed to originate from squared rings connecting the C_{60} molecules in the polymers. This feature is very weak in the spectrum recorded at 7.5 GPa. Furthermore, the same behavior can be seen for the split $H_g(1)$ mode at about 257 and 271 cm^{-1}. In fact, also most other H_g modes seem to be more intense in the quenched spectrum.

E. X-ray diffraction of a quenched sample

The results from the Raman analysis of the quenched material are in a good agreement with data obtained by synchrotron x-ray diffraction (XRD). An X-ray-diffraction image taken with a beam direction nearly parallel to the uniaxial direction of compression is shown in Fig. 8 together with a pattern integrated from this image. An analysis of the pattern shows that it could be indexed as a mixture of mainly ortho-

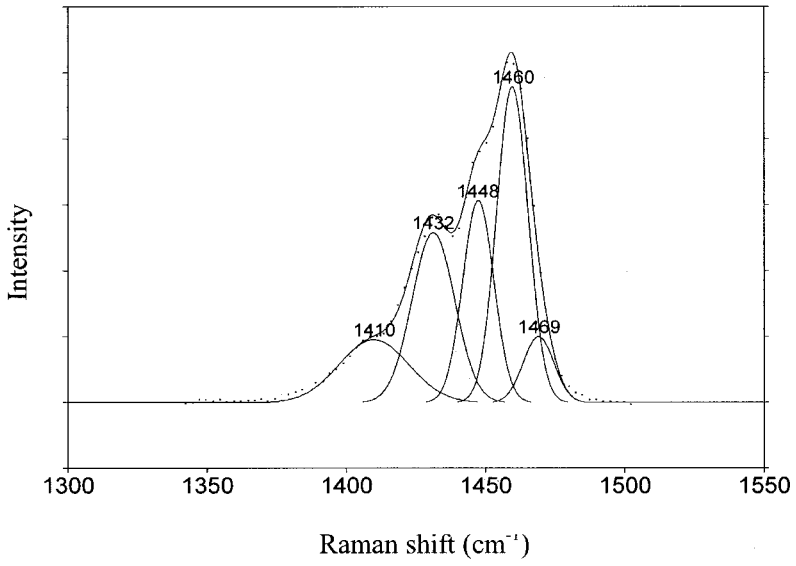

FIG. 7. Fitting of the spectrum of quenched sample in the spectral region around the $A_g(2)$ mode.

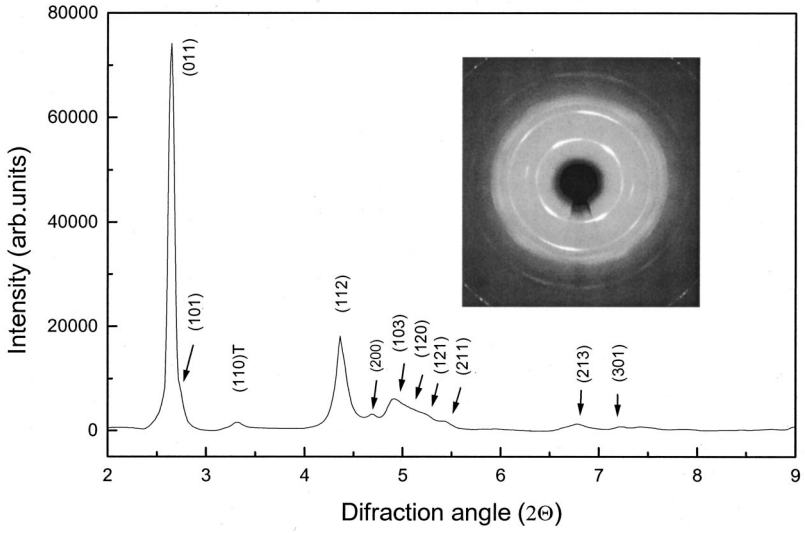

FIG. 8. XRD of a quenched sample obtained using synchrotron radiation: (a) integrated pattern, and (b) two-dimensional image. Peak indexes are shown for an orthorhombic structure with the exception of (110), which belongs to the tetragonal phase (labeled *T*).

rhombic phase together with some tetragonal phase. The cell parameters of the orthorhombic phase were determined to $a=9.08$ Å, $b=9.58$ Å, and $c=14.85$ Å using the 13 best peaks. These values are in good agreement with literature data. It should be noted, however, that the sample has a *b* axis, which is shorter than previously reported values of 9.8–10.0 Å.[4,18] The shortening of the *b* parameter can be explained by the partial tetragonal polymerization that is present as a disorder in the orthorhombic chain structure. Using a value 9.08 Å as a reference for the *b* parameter of the pure tetragonal phase and 9.9 Å for the pure orthorhombic phase, we could estimate a ratio of the orthorhombic to tetragonal phases of about 1.5. The 2D XRD patterns also showed a 6.44-Å line with two diffuse spots, which cannot be attributed to any reflections from the orthorhombic phase but identified as (110) reflections from the tetragonal (Fig. 8). Therefore, a tetragonal polymerization is present in our sample as a separate phase and as a disorder within the orthorhombic phase. The presence of a (104) reflection from the rhombohedral phase confirms the Raman data that this phase, together with the tetragonal phase, exists in small amounts in the quenched sample. The inset in Fig. 8 shows not only Debye-Scherrer rings but also several spots due to the preferential orientation of grains. The symmetrical position of these spots shows that the preferential orientation is correlated to the direction of pressurizing. The Debye-Scherrer ring with $d=8.09$ Å shows four spots which can be indexed as {011} reflections from the orthorhombic phase. The ring with $d=4.93$ Å shows six spots from the {112} reflections of the orthorhombic phase. Very diffuse and weak spots from {103} reflections of the orthorhombic phase can also be recognized. It is also interesting to note that we observed only two spots from {110} reflections of the tetragonal phase. Taking into account the non hydrostatic conditions of pressurizing in our experiment, the preferential orientation is rather probable and explains the observed pattern.

F. Construction of an *in situ P-T* diagram

The results from the Raman analysis have been summarized in a *P-T* diagram shown in Fig. 9. This diagram is in fact a diagonal section in the *P-T* space, and a number of such sections are required to construct a complete diagram

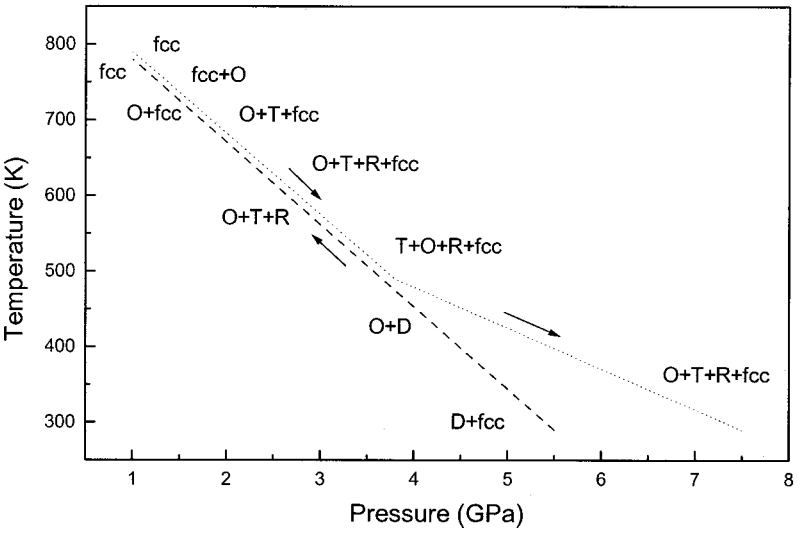

FIG. 9. *P-T* diagram showing phase transformations observed during the heating-cooling cycle. The phases are fcc, monomeric C_{60}; *D*, dimeric; *O*, orthorhombic; *T*, tetragonal; and *R*, rhombohedral. The phase with the highest intensity in the Raman spectra is listed first.

similar to that presented by, e.g., Sundqvist.[5] Nevertheless, the diagram allows us to compare the *in situ* experiments with previously published results obtained by *ex situ* experiments. In Fig. 9 the phase with the highest intensity of the $A_g(2)$ mode is listed first. This does not mean that this is the majority phase, since the cross sections of different polymeric phases are unknown and relative intensity can be used only for qualitative assessment.

The phase relations observed *in situ* in Fig. 9 and the *P-T* diagram based on *ex situ* data in Refs. 4, 5, and 8 show a very good general agreement, but some differences in details. This similarity is especially remarkable if we take into account that the *ex situ P-T* diagrams were based on data obtained at hydrostatic conditions, while we used nonhydrostatic conditions. First of all, we found no other phases besides those obtained in the *ex situ* studies. Heating from room temperature leads first to the formation of dimers (*D*) and one-dimensional orthorhombic polymers (*O*) and at $T > 470$ K (4.1 GPa) a mixture of the orthorhombic phase and two-dimensional tetragonal and rhombohedral phases ($O+T+R$) was observed. This seems to be a difference compared to the *ex situ P-T* diagram presented by Sundqvist, where only $T+R$ were observed together in the multiphase region.[5,8] Also we observed a formation of the dimeric polymer already at room temperature, which was continuously transformed to the orthorhombic phase at higher temperatures. This is a difference compared to the results presented by Sundqvist and co-workers where no region for a dimeric phase is given in the *P-T* diagrams,[5] although samples containing a dimeric polymer have been identified in later studies.[8] Our result is also different from the *P-T* diagram of Davydov *et al.*,[4] which shows a direct transition from dimeric phase to a tetragonal phase while no orthorhombic or rhombohedral phases were observed in this section of the *P-T* space. However, the transition lines in the *P-T* diagram presented by Davydov *et al.* are very approximate, and will fit to our data with only a small change in the slope of the lines.[4] Another difference can be seen above 670 K, where during both the heating and cooling steps we observed the one-dimensional orthorhombic phase. In contrast, the *ex situ P-T* diagram by Sundqvist suggests a direct transition from the monomeric fcc C_{60} phase at high temperature ($T > 500$ K, $P = 0-2$ GPa) to the two-dimensional *T* and *R* phases without the formation of any orthorhombic phase.[8] In this respect our observations are more similar to the *P-T* diagram presented by Davydov *et al.*, which shows an orthorhombic phase in the region around 550–750 K and 1–2 GPa. Therefore, our studies suggest that our results are complementary to the *P-T* diagrams presented by Sundqvist and co-workers[5,8] and Davydov *et al.*[4]

Another observation was that the phase composition during cooling was different than during the heating step. Much less amounts of the rhombohedral phase were observed during cooling compared to heating. This is in good agreement with previous studies, which observed that different pathways for applying pressure and temperature may lead to different proportions of polymeric phases.[4,8] Since we obtained, monomeric phase at the highest point of heating, the cooling half-cycle is similar to experiments where the temperature increase was followed by pressurization. Our results show that the preferential pathway for the preparation of the tetragonal phase is to start with a high temperature and then apply pressure (*T-P*) while the rhombohedral phase is favored by first applying pressure followed by a higher temperature (*P-T*). At present we have no explanation for the differences in the phase composition during the heating and cooling steps. It is possible, however, that kinetic constraints (e.g., orientational dynamics) in the polymerization process give rise to the observed differences.

Finally, an important question is whether the *in situ* data shown in Fig. 9 represent complete phase transformations phases or if prolonged heating could lead to a further change in phase composition. A test at 670 K showed that the intensities of the peaks from the orthorhombic phase reduced continuously with time. However, due to experimental difficulties with the high temperatures we were unable to stay longer than 1 h at this temperature, and it is possible that most or all of the orthorhombic phase may transform to tetragonal and rhombohedral polymers with prolonged heating. It should be noted that our heating times in general are longer than, or about equal to, those used in *ex situ* studies. It is therefore conceivable to assume that most of the *P-T* Diagrams reported in the literature are based on results where complete phase transformations have not been achieved. Therefore, Fig. 9 must be considered as a map of phases which appeared in our experiment. Nevertheless, we believe that it gives a better approximation of a true *P-T* diagram compared to the diagrams constructed using *ex situ* data.

IV. CONCLUDING REMARKS

In conclusion, *in situ* Raman spectroscopy data of C_{60} polymerization under HPHT conditions are presented. We have studied a diagonal section of a *P-T* diagram starting from room temperature and a pressure of 5.5 GPa heating the sample up to 780 K and 1 GPa, followed by a cooling of the sample back to room temperature and a pressure of 7.5 GPa. In general, the results are in a good general agreement with data obtained from *ex situ* studies. During the heating-cooling cycle, the polymerization order is monomeric $C_{60} \rightarrow$ dimeric $\rightarrow$ one-dimensional polymer (*O*) $\rightarrow$ two-dimensional polymers (*T,R*). Nevertheless, a preferential pathway to prepare the tetragonal (*T*) phase seems to be a high-temperature treatment followed by a pressure increase (*T-P*), and for the rhombohedral (*R*) phase a pressure treatment followed by high temperature. Also clear differences in the relative intensity for some modes were observed in the *in situ* and *ex situ* spectra.

ACKNOWLEDGMENTS

Financial support from the Swedish Natural Science Research Council (NFR) and the Swedish Research Council for Engineering Sciences (TFR) are gratefully acknowledged. Dr. J. Lindgren is also acknowledged for placing the Raman equipment at our disposal.

[1] M. Nunez-Regueiro, L. Marques, J.-L. Hodeau, O. Bethoux, and M. Perroux, Phys. Rev. Lett. **74**, 278 (1995).
[2] A. M. Rao, P. C. Eklund, J.-L. Hodeau, L. Marques, and M. Nunez-Regueiro, Phys. Rev. B **55**, 4766 (1997).
[3] V. A. Davydov, V. Agafonov, H. Allouchi, R. Ceolin, A. V. Dzyabchenko, and H. Szwarc, Synth. Met. **103**, 2415 (1999).
[4] V. A. Davydov, L. S. Kashevarova, A. V. Rakhmanina, V. M. Senyavin, R. Ceolin, H. Szwarc, H. Allouchi, and V. Agafonov, Phys. Rev. B **61**, 11 936 (2000).
[5] B. Sundqvist, Adv. Phys. **48**, 1 (1999).
[6] V. D. Blank, S. G. Buga, N. R. Serebryanaya, G. A. Dubitsky, S. N. Sulyanov, M. Yu. Popov, V. N. Denisov, A. N. Ivlev, and B. N. Martin, Phys. Lett. A **220**, 149 (1996).
[7] L. Marques, M. Mezouar, J.-L. Hodeau, M. Nunez-Regueiro, N. R. Serebriannaya, V. A. Ivdenko, V. D. Blank, and G. A. Dubitsky, Science **283**, 1720 (1999).
[8] R. Moret, P. Launois, T. Wågberg, and B. Sundqvist, Eur. Phys. J. B **15**, 253 (2000).
[9] S. M. Bennington, N. Kitamura, M. G. Cain, M. H. Lewis, R. A. Wood, A. K. Fukumi, and K. Funakoshi, J. Phys.: Condens. Matter **12**, L451 (2000).
[10] L. Marques, J. L. Hodeau, M. Nunez-Regueiro, and M. Perroux, Phys. Rev. B **54**, 12 633 (1996).
[11] A. V. Talyzin, L. S. Dubrovinsky, M. Oden, and U. Jansson, Diamond Relat. Mater. (to be published).
[12] S. J. Duclos, K. Brister, R. C. Haddon, A. R. Kortan, and F. A. Thiel, Nature (London) **351**, 380 (1991).
[13] E. Sterer, M. P. Pasternak, and R. D. Taylor, Rev. Sci. Instrum. **61**, 1117 (1990).
[14] S. Rekhi and L. S. Dubrovinsky, High Press-High Temp. **31**, 299 (1999).
[15] P. Nagel, V. Pasler, S. Lebedkin, A. Soldatov, C. Meingast, B. Sundqvist, P.-A. Persson, T. Tanaka, K. Komatsu, S. Buga, and A. Thaba, Phys. Rev. B **60**, 16 920 (1999).
[16] I. O. Bashkin, V. I. Raschupkin, A. F. Gurov, A. P. Moravsky, O. G. Rybchenko, N. P. Kobelev, Ya. M. Soifer, and E. G. Ponyatovsky, J. Phys.: Condens. Matter **6**, 7491 (1994).
[17] T. Wågberg, P. Jacobsson, and B. Sundqvist, Phys. Rev. B **60**, 4535 (1999).
[18] C. S. Sundar, P. Ch. Sahu, V. S. Sastry, G. V. Rao, V. Sridharan, M. Premila, A. Bharathi, Y. Hariharan, and T. S. Radhakrishnan, Phys. Rev. B **53**, 8180 (1996).